Low-Noise 0.8-0.96 and 0.96-1.12 THz Superconductor-Insulator-Superconductor Mixers for the Herschel Space Observatory

B. D. Jackson, G. de Lange, T. Zijlstra, M. Kroug, J. W. Kooi, J. A. Stern, and T. M. Klapwijk

***Abstract*— Heterodyne mixers incorporating Nb SIS junctions and NbTiN/SiO_2/Al microstrip tuning circuits offer the lowest-reported receiver noise temperatures to-date in the 0.8-0.96 and 0.96-1.12 THz frequency bands. In particular, improvements in the quality of the NbTiN ground plane of the SIS devices' on-chip microstrip tuning circuits have yielded significant improvements in the sensitivity of the 0.96-1.12 THz mixers relative to previously presented results. Additionally, an optimized RF design incorporating a reduced-height waveguide and suspended stripline RF choke filter offers significantly larger operating bandwidths than were obtained with mixers that incorporated full-height waveguides near 1 THz. Finally, the impact of junction current-density and quality on the performance of the 0.8-0.96 THz mixers is discussed and compared with measured mixer sensitivities, as are the relative sensitivities of the 0.8-0.96 and 0.96-1.12 THz mixers.**

***Index Terms*— Astronomical Satellites, Niobium, Niobium Compounds, Radio Astronomy, Submillimeter Wave Mixers, Superconductor-Insulator-Superconductor Mixers.**

I. Introduction

The Heterodyne Instrument for the Far-Infrared (HIFI) [1],[2] is a high-sensitivity, high-resolution heterodyne spectrometer that is being built for the European Space Agency's Herschel Space Observatory [3],[4]. The instrument's 0.48-1.25 and 1.41-1.91 THz frequency coverage will offer astronomers an unprecedented opportunity to observe a significant fraction of the sub-millimeter and far-infrared spectrum, much of which is not observable from ground-based telescopes due to absorption by atmospheric water vapor. In order to take full advantage of this space-based observatory, the HIFI instrument will incorporate state-of-the-art cryogenic heterodyne mixers, with five superconductor-insulator-superconductor (SIS) mixers covering the 0.48-1.25 THz band and two hot-electron bolometer (HEB) mixers covering 1.41-1.91 THz.

Unfortunately, although traditional Nb SIS mixers offer quantum-limited sensitivities below 0.7 THz [5]-[7], increasing resistive losses in their Nb-based microstrip transmission lines at frequencies above the "gap frequency" of Niobium ($F_{gap,Nb} = 2\Delta_{Nb}/h \sim 0.7$ THz) [8] cause the sensitivities of these mixers to drop significantly above 0.7 THz [9]. However, previous work has shown that the use of NbTiN[1]-based microstrip RF tuning circuits allows the sensitivity of 0.75-1.0 THz SIS mixers to be significantly improved [10]-[12]. Furthermore, as is discussed in more detail in [13], the integration of Nb SIS junctions with a NbTiN/SiO_2/Al microstrip tuning circuit in which the NbTiN ground plane is deposited at 400ºC (in place of the room-temperature-deposited films used previously) allows low-noise SIS mixer operation to be extended to at least 1.12 THz.

Following from these advances, this paper describes the RF design and performance of the 0.8-0.96 and 0.96-1.12 THz mixers that have been developed for use in Bands 3 and 4 of the HIFI instrument. In particular, this paper discusses the integrated designs of reduced-height waveguide embedding circuits and two-junction SIS tuning circuits that yield efficient coupling of radiation to the mixers' SIS junctions over each frequency band. Additionally, the impact of the current-densities and leakage currents of the SIS junctions on their mixing performance is discussed in light of simulations of the heterodyne performance of the mixers' two-junction tuning circuits. This mixer model is also used to compare the relative performance of the 0.8-0.96 and 0.96-1.12 THz mixers.

Manuscript received January 26, 2005. The work presented here was partially supported by the Technologiestichting STW (of the Netherlands), the Nederlandse Organisatie voor Wetenschappelijk Onderzoek, and the European Space Agency (via ESTEC Research Contract No. 11653/95).

B. D. Jackson is with the SRON National Institute for Space Research, Landleven 12, 9747 AD Groningen, The Netherlands and the Kavli Institute of Nanoscience, Faculty of Applied Sciences, Delft University of Technology, Lorentzweg 1, 2628 CJ Delft, The Netherlands. (Corresponding author: B. D. Jackson, phone: +31-50-363-8935; fax: +31-50-363-4033; e-mail: B.D.Jackson@sron.rug.nl)

G. de Lange is with the SRON National Institute for Space Research, Landleven 12, 9747 AD Groningen, The Netherlands. (e-mail: G.de.Lange@sron.rug.nl)

T. Zijlstra, M. Kroug, and T. M. Klapwijk are with the Kavli Institute of Nanoscience, Faculty of Applied Sciences, Delft University of Technology, Lorentzweg 1, 2628 CJ Delft, The Netherlands. (e-mail: zijlstra@dimes.tudelft.nl, kroug@dimes.tudelft.nl, t.m.klapwijk@tnw.tudelft.nl)

J. Kooi is with the California Institute of Technology 320-47, Pasadena, CA 91125, USA. (e-mail: kooi@submm.caltech.edu)

J. A. Stern is with the Jet Propulsion Laboratory, California Institute of Technology, 4800 Oak Grove Drive, Pasadena, CA 91109, USA. (e-mail: Jeffrey.Stern@jpl.nasa.gov)

[1] For simplicity, the compound $Nb_{1-x}Ti_xN_{1-\delta}$, where $x = 0.3$ and $\delta = 0$, is referred to as NbTiN throughout this paper.

The opto-mechanical designs of these mixers (including their corrugated horns), in addition to the designs of their Intermediate Frequency output coupling circuits and their shielding from external electromagnetic interference are described elsewhere [14].

II. Mixer and SIS Device Design

Previous reports of the development of NbTiN-based SIS mixers made use of two basic mixer geometries: a quasioptical mixer incorporating a 0.95 THz twin-slot antenna (see [11]) and a waveguide mixer incorporating a full-height 1 THz waveguide (see [12]). These results demonstrated that a NbTiN/SiO_2/Al microstrip RF matching network can be integrated with "standard" 1 μm^2 Nb/Al-AlO_x/Nb SIS junctions to yield low receiver noise temperatures up to 1 THz (and [13] demonstrates that this region of low-noise operation may be extended to at least 1.12 THz by the use of a NbTiN ground plane that is deposited at 400ºC). However, the fixed-tuned RF bandwidth of the 1 THz waveguide mixer in [12] was limited to ~ 100 GHz, whereas the quasioptical mixer in [11] offered fixed-tuned bandwidths of ~ 200 GHz. This limitation of the previously demonstrated waveguide mixer has been addressed by a redesign of the waveguide embedding geometry [15] and the SIS device's on-chip microstrip tuning circuit to optimize the coupling to the SIS junctions.

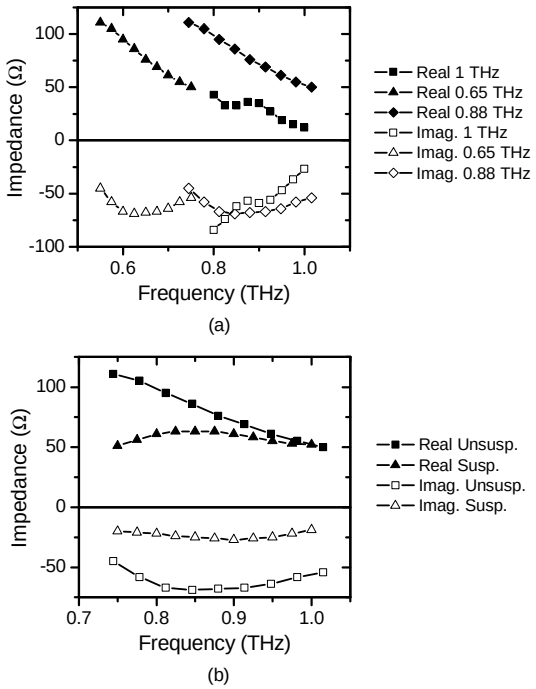

Fig. 1 – Effective source impedance at the input to the on-chip microstrip tuning circuit (at the center of the "across the waveguide" bowtie probe, given the fixed-depth waveguide backshort, the fused quartz substrate in the substrate channel, and the RF choke filter patterned on the substrate surface). (a) A comparison of the full-height 1 THz waveguide geometry and the half-height 0.65 THz waveguide geometries used previously with the "unsuspended" half-height 0.88 THz design. (b) A comparison of half-height 0.88 THz waveguide geometries with suspended and unsuspended quartz substrates in the substrate channel. The geometries of the mixers analyzed here are summarized in Table I.

The starting point of this redesign was a move from the full-height 1 THz waveguide geometry that was used in [12] to scaled versions of the 0.65 THz half-height waveguide geometry that was used in mixers produced for the James Clerk Maxwell Telescope, in Hawaii [16],[17]. In particular, for each of these designs, Fig. 1(a) presents the effective source impedance at the input to the on-chip microstrip tuning circuit that is produced by a combination of the waveguide, the fixed-depth waveguide backshort, the fused quartz substrate in the substrate channel (including the RF choke filter on the substrate), and the "across the waveguide" bowtie probe. (This "source impedance" has been calculated in a 3-dimensional electromagnetic field simulator [18].) From this plot, it is seen that the original 1 THz waveguide design is characterized by a source impedance with a strong frequency-dependence and a large imaginary component. In comparison, the source impedances of the 0.65 and 0.88 THz half-height waveguide designs are much less frequency-dependent (although they retain significant reactive components).

Further "improvements" in the source impedance offered by the waveguide embedding design are obtained by suspending the SIS device substrate in the substrate channel (and fine-tuning the dimensions in the RF choke filter to re-center the passband of the filter on the center frequency of the design). As is seen in Fig. 1(b), this further reduces the frequency-dependence and reactance of the source impedance at the input of the on-chip tuning circuit. (For clarity, only the results for the 0.88 THz design are shown here – the 1.04 THz design is a scaled version of the 0.88 THz design.)

Finally, the RF designs of the mixers were completed by optimizing the geometry of the twin-junction tuning circuit used in [12] (see Fig. 2) to maximize the coupling of incident RF power to the SIS junctions over the 0.8-0.96 and 0.96-1.12 THz bands, given the frequency-dependent source impedances in Fig. 1. The resulting coupling to the SIS junctions is plotted in Fig. 3 for several combinations of waveguide embedding geometry and SIS device parameters (which are summarized in Tables I and II, respectively).

A number of features are clearly identifiable in these results. First, it is seen that with a moderate junction current-density (J_c = 8 kA/cm^2), the "suspended" and "unsuspended" 0.88 THz designs offer similar coupling efficiencies (50-60%

Table 1
Waveguide mixer embedding geometries analyzed in Fig. 1.

Design	waveguide *W* x *H*	backshort depth	substrate channel *W* x *D*	substrate [b] *W* x *T*
1 THz	120 x 240	60	90 x 75	70 x 40
650 GHz	100 x 400	80	100 x 75	80 x 40
0.88 THz	74 x 296 [a]	60	75 x 55	60 x 30
0.88 THz suspended	74 x 296 [a]	25	90 x 87	75 x 45 [c]

all dimensions are given in µm, *W* = width, *D* = Depth, *H* = Height

[a] dimensions used in modeling, actual dimensions are 75 µm x 300 µm and 60 µm x 240 µm

[b] polished fused quartz, ε_r = 3.8, *T* = the substrate thickness after thinning (by polishing)

[c] suspended by 17 µm above the bottom of the substrate channel

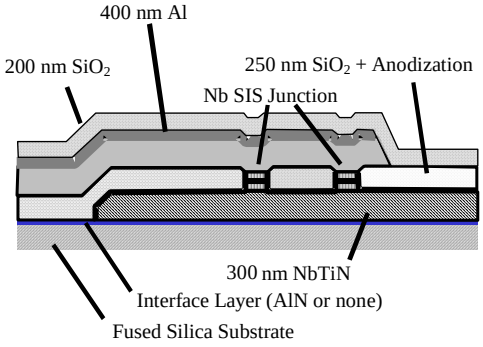

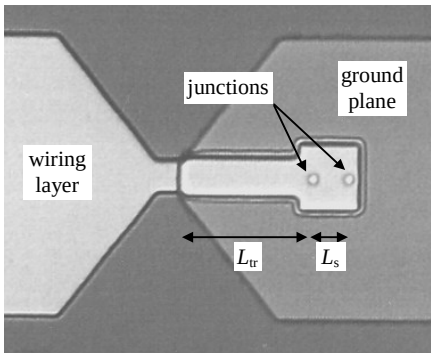

Fig. 2 – The twin-junction SIS tuning circuit geometry: (a) a photograph of a 1 THz mixer device (adapted from [12]) and (b) a schematic cross-section of the tuning circuit layer structure (adapted from [11]).

across the 0.8-0.96 THz band, with the "unsuspended" design actually offering slightly higher efficiencies). Moving to a higher current-density (J_c = 15 kA/cm^2) significantly improves the coupling to the junctions (due to the junctions' reduced ωRC product), and the coupling obtained with the "suspended" design is slightly better than that obtained with the "unsuspended" design. Beyond this, Fig. 3(b) demonstrates that the coupling to the junctions in the 1.04 THz design is strongly dependent upon the properties of the NbTiN ground plane – the use of a film deposited at room-temperature is expected to result in a strong drop in coupling above ~ 1 THz (see [11] and [12]), whereas the use of a film deposited at 400ºC should offer strong coupling over the full 0.96-1.12 THz band (see [13]).

Based upon these calculations, SIS mixers with three combinations of junction current-density, NbTiN quality (superconducting transition temperature, $T_{c,NbTiN}$, and low-temperature normal-state resistivity, $\rho_{n,20K}$), and embedding geometry have been produced. Two 0.88 THz mixers (incorporating junctions with J_c = 6.5 and 13 kA/cm^2, $T_{c,NbTiN}$ = 14.4 K, $\rho_{n,20K}$ = 110 μΩ·cm and a suspended embedding geometry) have been produced for Band 3 of the HIFI instrument. Similarly, a 1.04 THz mixer incorporating a suspended-substrate waveguide geometry with J_c = 6.5 kA/cm^2, $T_{c,NbTiN}$ = 16 K, and $\rho_{n,20K}$ = 60 μΩ·cm has been produced for Band 4 of HIFI. In all cases, the SIS junctions are Nb/Al-AlO$_x$/Nb tunnel junctions with A ~ 1 μm^2. The microstrip transmission lines combine a 400 nm NbTiN ground plane, a 250 nm SiO$_2$ dielectric layer (with a nominal ε_r = 3.8), and a 400 nm Al wiring layer (with a low-temperature DC conductivity of $\sigma_{Al,4K}$ = 2-3 x 10^8 Ω^{-1}m^{-1}).

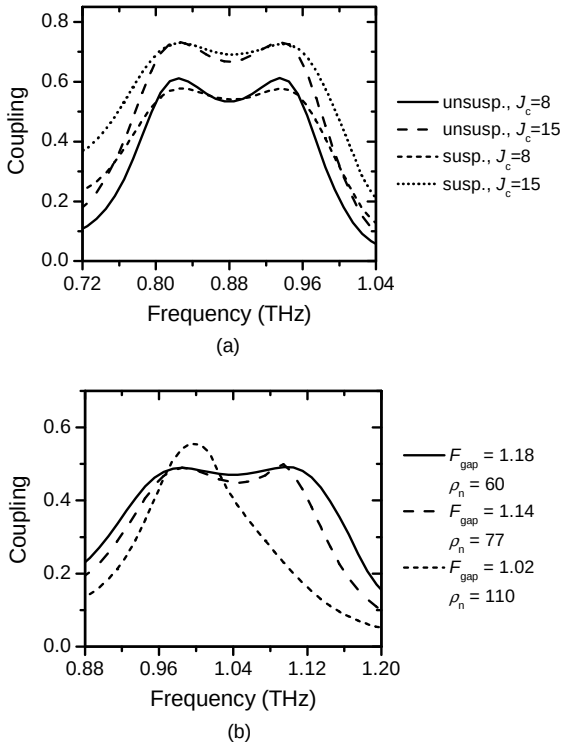

Fig. 3 – (a) Calculated coupling to the SIS junctions for twin-junction SIS devices mounted in half-height 0.88 THz waveguides with suspended and unsuspended substrates. A slight benefit is obtained from the suspended substrate design if high current-density junctions are used (the values of J_c in the legend are given in kA/cm^2). (b) Calculated coupling to suspended-substrate twin-junction SIS devices mounted in a half-height 1.04 THz waveguide. A clear dependence of the RF coupling on the superconducting properties of the NbTiN ground plane is observed. Note that the values given the legends are the "gap frequency" and low-temperature normal-state resistivity of NbTiN in THz and μΩ·cm, respectively ($F_{gap,NbTiN} = 2\Delta_{NbTiN}/h$).

The fabrication and performance of these mixers are described and discussed further in the following Sections.

III. SIS Device Fabrication

The SIS devices used here were produced using a process that is derived from that which was used for the demonstrations of quasioptical and waveguide mixers incorporating NbTiN/SiO$_2$/Al tuning circuits (see [11] and [12], respectively). However, a number of significant modifications to the process have been made in order to improve the patterning of the SIS junctions and the Al wiring layer, and to incorporate higher-quality NbTiN ground planes in the 1.04 THz mixers.

The primary modifications to the junction definition process have been: (1) to move from a CF$_4$+O$_2$ gas mixture to SF$_6$+O$_2$ for the reactive ion etching of the Nb junction electrodes (to improve the anisotropy and repeatability of the etch); and (2) to add an O$_2$ plasma etch of the resist pattern following the etch of the top Nb junction electrode (prior to Ar sputter etching the Al-AlO$_x$ barrier and reactive ion etching the bottom Nb electrode). As is discussed in [13], this "resist

TABLE II
SIS JUNCTION AND NBTIN GROUND PLANE CHARACTERISTICS AND TUNING CIRCUIT GEOMETRIES OF THE SIS DEVICES DISCUSSED HERE.

Batch Label Device Number	880 low-J_c c78, c87	880 high-J_c c20, c78	1040 c22, f49
Waveguide	0.88 THz	0.88 THz	1.04 THz
Embedding Design	suspended	suspended	suspended
Junction			
A (μm^2)	0.9, 1.1	0.9	1.15, 1.05
J_c (kA/cm^2)	6.5	13	6.5
$R_{2.0mV}/R_N$	60	20	30-50
NbTiN			
$T_{deposition}$ (ºC)	20	20	400
T_c (K)	14.4	14.4	16
$\rho_{n,20K}$ ($\mu\Omega$·cm)	110	110	60
Separation			
L (μm)	5.5	5.5	5.5, 3.5
W (μm)	6-7	6-7	6-7
Transformer			
L (μm)	24, 27	24	22, 20
W (μm)	5-6	5-6	4, 5

recessing" step yields a stepped junction profile in which the edges of the active portion of the Al-AlO_x barrier are not exposed to the Ar sputter etch of the barrier, since the final size of the top electrode is reached at the completion of the bottom electrode etch. This is expected to improve the quality of a typical junction (i.e. to reduce its leakage current) by reducing the risk of damage to the tunnel barrier during the etch process.

On top of these changes to the junction definition step, the other significant changes to the SIS device process have been: (1) using a chlorine-based reactive ion etch to pattern the Al wiring layer (which offers improved dimension control relative to the lift-off process that was used in [11] and [12]); and (2) using NbTiN ground planes deposited at 400ºC (at NASA's Jet Propulsion Laboratory [19]) in the 1.04 THz mixers. Finally, because the lift-off process that was used previously cannot be used to pattern ground planes that are deposited at high temperatures, these films were patterned by reactive ion etching in SF_6+O_2.

As in [11] and [12], contact UV lithography is used for all resist pattern definition, RF magnetron sputtering is used to deposit the SiO_2 dielectric and passivation layers, and DC magnetron sputtering is used to deposit the Nb, NbTiN, and Al layers.

Table II summarizes the material characteristics and tuning circuit geometries of the SIS devices that are discussed in the Sections that follow.

IV. DC CURRENT-VOLTAGE CHARACTERISTICS

Fig. 4 presents the bias current and IF output power as a function of bias voltage for two SIS devices (one 0.88 THz device with J_c = 13 kA/cm^2 and one 1.04 THz device with J_c = 6.5 kA/cm^2). In general, the junction qualities of these devices, as measured by their sub-gap to normal-state resistance ratios ($R_{2.0mV}/R_N$), are excellent, with $R_{2.0mV}/R_N$ = 30-60 for devices with J_c = 6.5 kA/cm^2 and $R_{2.0mV}/R_N$ ~ 20 for devices with J_c = 13 kA/cm^2 (at a mixer temperature of 2-2.5 K).

Beyond this, two other features are noted in Fig. 4. First, the photon-step in the 1.04 THz device pumped at 1.14 THz is barely wide enough to yield a bias point that is not affected by the Shapiro effect (which can cause instabilities in the IF output power in the output power peaks seen on either side of $V_{Shapiro} = hF_{LO}/2e$ = 2.1 mV/THz). Additionally, whereas the 0.88 THz devices have a typical series resistance in their Al wiring layer of 0.7 Ω (which is consistent with the low-temperature DC resistivity of the Al film), the 1.04 THz devices have a series resistance of 1.5 Ω. This indicates that the resistivity of the Al wiring layer is somewhat higher in the 1.04 THz devices than the $\sigma_{Al,4K}$ ~ 2.5x10^8 $\Omega^{-1}m^{-1}$ that is assumed in the design.

V. RF MEASUREMENT SETUP

The heterodyne sensitivities of the mixers described here have been obtained from conventional Y-factor measurements using a room-temperature "hot" blackbody signal source and a 77 K "cold" blackbody source (using the Callen-Welton formulation [20] to determine their effective source

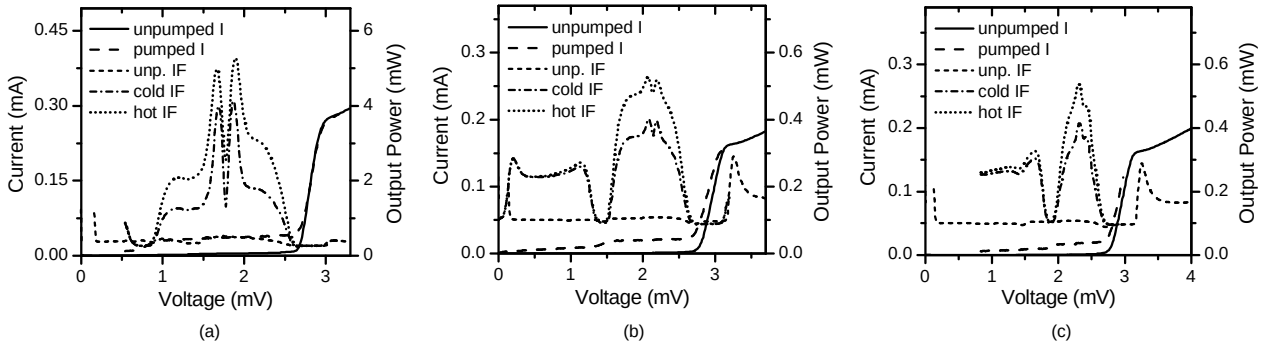

Fig. 4 – (a) Bias current and mixer IF output power as a function of bias voltage for a 0.88 THz SIS tunnel junction with a current-density of J_c = 13 kA/cm^2, operated at 0.86 THz. (b,c) Bias current and mixer IF output power as a function of bias voltage for a 1.04 THz SIS junction with J_c = 6.5 kA/cm^2, operated at 1.02 THz (in (b)) and 1.14 THz (in (c)). The limited bias range that remains in the 1.04 THz device pumped at 1.14 THz is noted – this is close to the maximum operating frequency for a "traditional" Nb/Al-AlO_x/Nb SIS junction. In both cases, the junction qualities (as measured by their sub-gap to normal-state resistance ratios) are excellent, with $R_{2.0mV}/R_N$ = 30-60 and 20 obtained for J_c = 6.5 and 13 kA/cm^2, respectively. (Note that (b) is adapted from [13].)

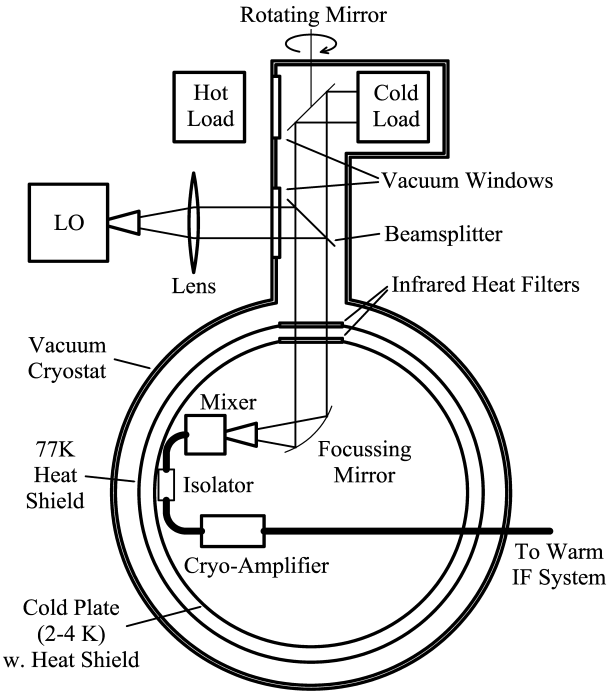

Fig. 5 – A schematic representation of the mixer test receiver. This includes a vacuum hot-cold load that is used to improve the accuracy of measurements of the mixer sensitivity by removing the vacuum window from the optical path to the liquid-nitrogen-cooled cold load, and by eliminating the influence of atmospheric absorption of sub-millimeter radiation on the noise measurements.

temperatures from their physical temperatures). Furthermore, because this work is focused on the development of mixers for the HIFI instrument (which includes a window-free, all-reflective optical design) an attempt has been made to minimize the receiver's input coupling losses by: (1) replacing the dielectric focusing lens used previously with a Au-coated mirror on the 4K stage of the liquid-helium-cooled test cryostat; and (2) making use of a vacuum hot-cold load. In particular, using this vacuum hot-cold load removes the cryostat's vacuum window from the optical path between the mixer and the cold load, and eliminates the effect of absorption by atmospheric water vapor, which can be significant at sub-millimeter wavelengths. Fig. 5 presents a schematic representation of the mixer test system, including the vacuum hot-cold load, in which a rotating mirror located inside the cryostat is used to chop between the hot load (a room-temperature absorber located outside the cryostat) and the cold load (the "blackened" bottom of a liquid nitrogen vessel built into the receiver's vacuum system).

Differences between the mixer test system and the environment of the HIFI instrument have been further minimized by the use of a cryogenic intermediate frequency (IF) amplification system that includes prototypes of the cryogenic 4-8 GHz isolator and low-noise amplifier used in the HIFI instrument (from PamTech [21], and the Centro Astronomico de Yebes [22], respectively). Furthermore, the SIS devices have been tested in prototypes of the mixer blocks that will be used in the instrument's 0.88 and 1.04 THz bands (see [14]), at an operating temperature of 2-2.5 K (which is close to the expected operating temperature of the mixers in the instrument). (This low operating temperature is reached by pumping on the cryostat's helium bath.)

In reporting the receiver sensitivities presented here, two values are generally given: $T_{N,rec}$, the measured double side-band (DSB) receiver sensitivity obtained with the mixer mounted in the test receiver (averaged over the full 4-8 GHz IF band); and $T_{N,mixer+IF}$, the effective input noise of the mixer and the IF amplifier system (which is obtained by correcting the measured receiver noise temperatures for the calculated/measured losses in the 14 or 49 µm Mylar beamsplitter and the Zitex G104 infrared heat-filters).

Finally, the mixers' direct-detection sensitivities are also presented here because they provide a snapshot of the frequency-dependence of the coupling of radiation from an incident optical beam to the SIS junctions. These results have been obtained with a Fourier transform spectrometer in which an evacuated Michelson interferometer is used as a tunable signal source that is injected into the mixer test cryostat via the optical window through which the "hot" signal passes in

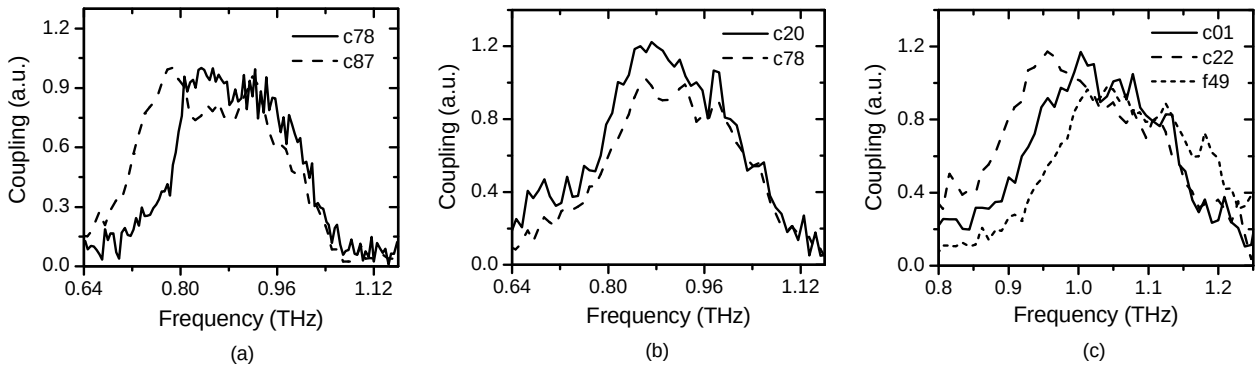

Fig. 6 – Direct-detection sensitivities of several SIS devices mounted in the 0.88 THz and 1.04 THz mixer blocks. In all cases, the embedding geometry is a half-height waveguide design with the substrate suspended in the substrate channel. (a) Results for 0.88 THz mixers with junction current-densities of J_c = 6.5 kA/cm^2. (b) Results for 0.88 THz mixers with J_c = 13 kA/cm^2. (c) Results for 1.04 THz mixers with J_c = 6.5 kA/cm^2. In each case, strong coupling over a broad RF bandwidth is obtained (although the center-frequency and the frequency-dependence of the response is dependent on the tuning circuit geometry and junction size). The geometries of these devices are summarized in Table II, using the device labels identified in the legend of each figure.

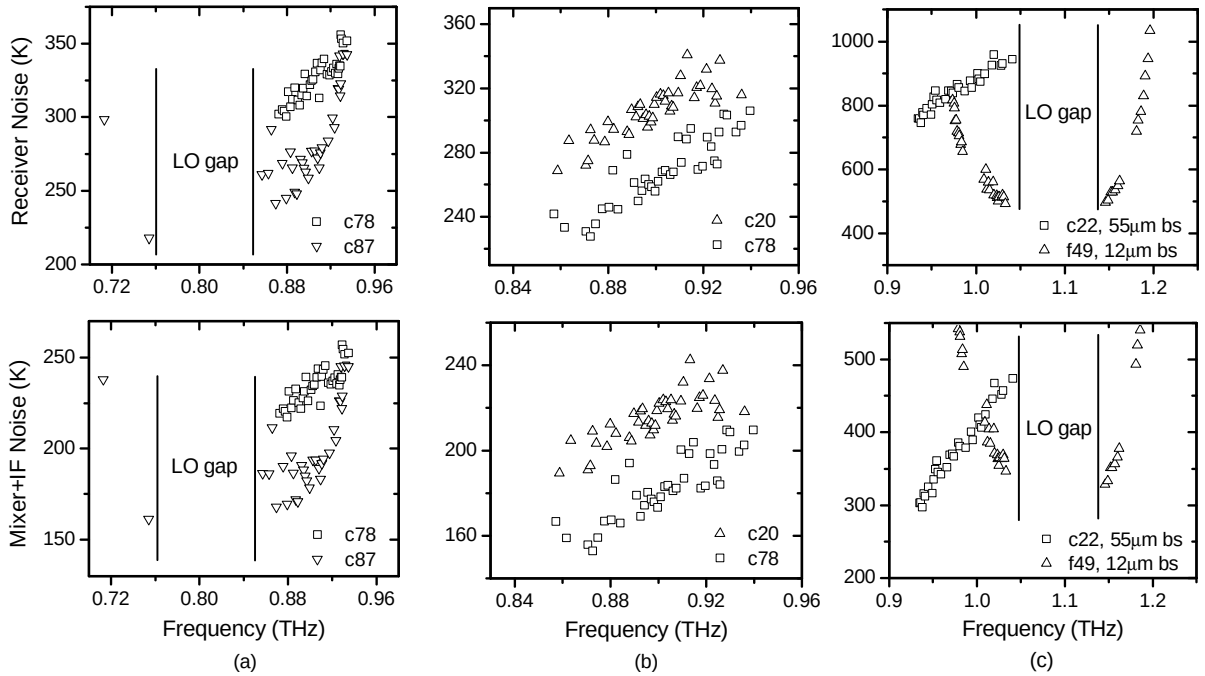

Fig. 7 – Measured double side-band receiver noise temperatures ($T_{N,rec}$) for several of the devices/mixers whose direct-detection (FTS) sensitivities are plotted in Fig. 6. The effective input noise temperatures of the combination of the mixers and IF system ($T_{N,mixer+IF}$) (obtained by correcting the measured receiver sensitivities for the calculated/measured losses in the receiver optics), are also shown. All of these measurements are performed at mixer temperatures of 2-2.5 K, averaging over the full bandwidth of a 4-8 GHz IF system with $T_{N,IF}$ ~ 8-10 K. (a) Results for 0.88 THz mixers with J_c = 6.5 kA/cm^2. (b) Results for 0.88 THz mixers with J_c = 13 kA/cm^2. (c) Results for 1.04 THz mixers with J_c = 6.5 kA/cm^2. In each case, high sensitivity over a broad RF bandwidth is obtained (although the center-frequency and the frequency-dependence of the response is dependent on the tuning circuit geometry and junction size). The geometries of these devices are summarized in Table II using the device labels indicated in the legends in the bottom right corner of each figure.

heterodyne sensitivity measurements. In order to allow the measured results to be compared with the calculated coupling efficiencies, the measured spectra have been corrected for a standing wave in the output of the Michelson interferometer (with a period of ~ 70 GHz and a peak-to-peak amplitude of 0.8 dB), and have been multiplied by a factor of F (in THz) to account for the fact that the measured spectra are proportional to the photon detection efficiency, while the calculated spectra are of the power coupling.

VI. RF Measurement Results

Fig. 6 presents the direct-detection sensitivities of several SIS devices in each of the three mixers discussed here (the 0.88 THz mixer with moderate- and high-J_c junctions and the 1.04 THz mixer with moderate-J_c junctions). From these results, it is seen that both current-densities yield efficient coupling to the SIS junctions over broad RF bandwidths. Furthermore, provided that the response is properly centered on the target band (i.e. by properly matching the junction sizes to the tuning circuit geometries), efficient coupling can be obtained over the full 0.8-0.96 and 0.96-1.12 THz bands.

Following the direct-detection sensitivities, Fig. 7 presents measured heterodyne sensitivities of several of the SIS devices whose direct-detection sensitivities are plotted in Fig. 6. From these results, it is observed that the 0.88 THz mixers yield $T_{N,rec}$ = 300 K and $T_{N,mixer+IF}$ = 200 K, or better, across most of the 0.8-0.96 THz band. The 1.04 THz mixers yield $T_{N,rec}$ = 500 K and $T_{N,mixer+IF}$ = 400 K, or better, across most of the 0.96-1.12 THz band. Furthermore, a number of additional observations can be made: (1) the sensitivities of the 0.88 THz mixers incorporating 6.5 and 13 kA/cm^2 junctions are similar (given the device-to-device variability of their sensitivities); (2) as is discussed further in [13], the use of a NbTiN ground plane deposited at 400ºC yields sensitive SIS mixers for frequencies up to at least 1.12 THz; and (3) the input noise temperatures of the 1.04 THz mixers are ~ 40-50% higher than those of the 0.88 THz mixers.

The wider RF bandwidths that are expected from the use of higher current-density junctions (see Fig. 3) are not immediately obvious in the measured results in Fig. 6 and 7. However, this may be partly due to the 1 THz "gap frequency" of the NbTiN ground plane limiting the mixers' high-frequency performance (since the devices presented here have been selected to have strong responses in the 0.8-0.96 or 0.96-1.12 THz bands, as opposed to maximum bandwidth).

VII. Discussion

A. Twin-Junction Mixer and Receiver Noise Model

Calculations of the coupling of radiation to the SIS junctions clearly show that the coupling efficiency increases significantly with increasing current-density (from ~ 55% at J_c = 8 kA/cm^2 to ~ 70% at J_c = 15 kA/cm^2 for the 0.88 THz

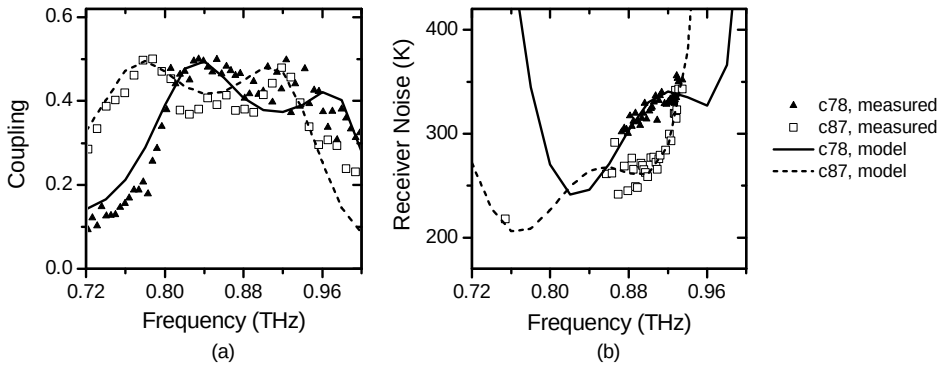

Fig. 8 – Comparison of the measured and calculated direct-detection sensitivities and receiver noise temperatures for devices c78 and c87 from the low-J_c 0.88 THz mixer (with J_c = 6.5 kA/cm^2 and $R_{2.0mV}/R_N$ = 60). Note that the tuning circuit dimensions in the calculations have been tuned slightly to match the frequency-dependences of the measured direct-detection sensitivities. Matching the magnitudes of the calculated and measured noise temperatures requires that a 2.8-dB loss be inserted in the model, in front of the mixer, at a physical temperature of 2.5 K.

mixer design). However, measurements of the heterodyne sensitivities of devices with J_c = 6.5 and 13 kA/cm^2 show no significant difference in performance. This may be attributed to the fact that the leakage currents of the higher current-density junctions are higher than those of the lower current-density junctions ($R_{2.0mV}/R_N$ ~ 20 in place of 30-60). In particular, the larger leakage currents apparently generate sufficient additional shot-noise to counteract the improved coupling of radiation to the junctions. (Note that the "sharpness" of the current-voltage characteristics of the lower and higher current-density devices in Fig. 4 is effectively the same, after correcting for the series resistance in their wiring layers – dV_{gap} ~ 0.1-0.2 mV.)

This conclusion is supported by an analysis of the heterodyne performance of the twin-junction tuning circuit. In this analysis, each of the microstrip transmission line sections in the RF tuning circuit is replaced by a π-matrix lumped-element circuit model and the coupling of LO power to the two junctions is then determined in an iterative calculation that takes into account the dependence of the junction admittances on the absorbed LO powers. Given the (different) LO power coupling to the two junctions, the junctions are then replaced by 3-port Tucker admittance and noise correlation matrices [23] in order to generate a 3-port model for the complete tuning circuit, from which the frequency-dependent mixer noise and gain can be determined. In order to evaluate the impact of the junction quality and current-density on the mixer noise, the junction models are modified by adding a parallel resistance to the measured current-voltage characteristic of a junction with J_c = 6.5 kA/cm^2 and $R_{2.0mV}/R_N$ = 60, and then scaling the voltage and current to obtain the desired gap voltage and junction resistance. (Note that adding this parallel resistance does not change the "sharpness" of the current step and the junction's gap voltage, as is the case in the mixers discussed here.) Finally, the shot-noise that is produced by this "excess leakage current" is multiplied by the bias-voltage-dependent factor that was developed in [24] and [25] to account for the amplification of shot-noise by multiple Andreev reflection in the leakage current of "leaky" SIS junctions (this factor is ~ 2.3 at V_{bias} = 2.2 mV).

Fig. 8 presents a comparison of the measured and calculated RF coupling and receiver noise for two 0.88 THz devices with different junction resistances and tuning circuit dimensions. Because the tuning circuit dimensions and material properties are not known with absolute certainty, the tuning circuit dimensions have been fine-tuned to match the frequency-dependence of the calculated RF coupling efficiencies to the measured direct-detection sensitivities (applying the same corrections to the geometries of both devices). Furthermore, an excess noise term is added to the calculated receiver noise to match the measured noise temperatures – for the sake of argument, this excess noise is represented as a 2.8 dB loss in front of the mixer, at a physical temperature of 2.5 K. As is seen in Fig. 8, the result is a reasonably consistent match between the measured and calculated receiver sensitivities for the two mixers.

The observed excess noise/loss may originate from a number of sources, including the 77K blackbody load not being perfectly black; excess losses in the receiver optics; losses in the corrugated horn, waveguide, and/or substrate channel due to manufacturing errors and/or resistive losses that are not included in the model; dielectric losses in the fused quartz substrate and/or the SiO_2 dielectric layer in the tuning circuit, both of which are assumed to be loss-less; excess resistive losses in the Al wiring layer and/or the NbTiN ground plane; resistive losses in the Nb junction electrodes (which are not taken into account in this model, but which are present); and impedance mismatches and/or resistive losses in the mixer's IF circuit (which is represented by a 50 Ω load and an input noise of 10 K).

B. Junction Current-Density and Quality vs. Receiver Noise

Using the previously described receiver noise model of the twin-junction mixer, including the 2.8 dB excess noise term that was determined from the results in Fig. 8, the receiver noise of the 0.88 THz mixer has been calculated as a function of junction current-density and quality (while adjusting the tuning circuit dimensions to optimize the average RF coupling efficiency over the 0.8-0.96 THz band for each case). The

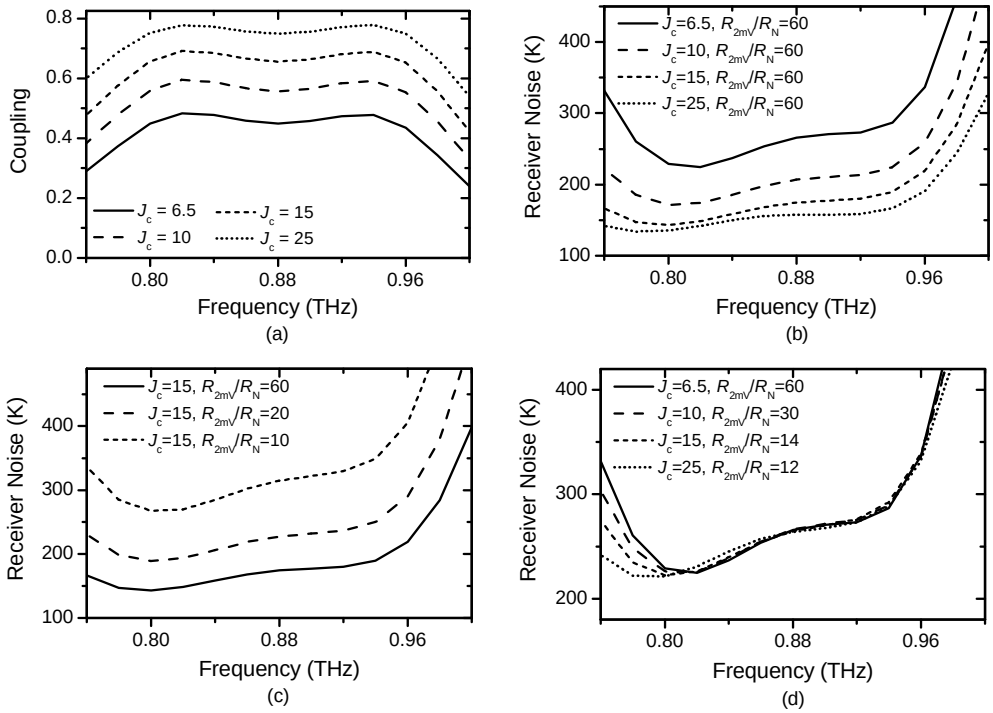

Fig. 9 – Calculated sensitivities of 0.88 THz SIS mixers with twin-junction NbTiN/SiO_2/Al tuning circuits and junction current-densities ranging from 6.5 to 15 kA/cm^2. The same noise and gain contributions for the receiver optics and IF system that were used in Fig. 8 are used in these calculations (including the 2.8-dB excess loss in front of the mixer). (a) Frequency-dependence of the direct-detection coupling to the SIS junctions for different current-densities. (b,c) Frequency-dependence of the DSB receiver noise for different combinations of current-density and junction quality ($R_{2.0mV}/R_N$). (d) Frequency-dependence of the DSB receiver noise for different current-densities, with the junction quality being defined at each current-density as the value that is needed to obtain the same sensitivity as is obtained with J_c = 6.5 kA/cm^2 and $R_{2.0mV}/R_N$ = 60.

results of these calculations are summarized in Fig. 9.

Not surprisingly, it is seen that if the junction-quality ($R_{2.0mV}/R_N$) remains constant, the receiver noise temperature drops significantly with increasing current-density (see Fig. 9(b)). However, experience shows that junction quality drops with increasing current-density in high current-density (J_c > 10-15 kA/cm^2) SIS junctions with AlO_x tunnel barriers. This reduction in junction quality causes a corresponding increase in mixer shot-noise [24],[25] that will (partially) offset the improved coupling of incident radiation to the junctions (see Fig. 9(c)). Indeed, Fig. 9(d) presents the calculated receiver sensitivities for current-densities between 6.5 and 15 kA/cm^2, with a junction quality in each case that is defined as the minimum value that is needed for junctions with that current-density to offer a receiver sensitivity that is equal to that which is obtained with J_c = 6.5 kA/cm^2 and $R_{2.0mV}/R_N$ = 60 kA/cm^2.

Reviewing these calculations, it is noted that moving from J_c = 6.5 to 10 and 15 kA/cm^2 requires that junction qualities of at least $R_{2.0mV}/R_N$ = 30 and 14, respectively, are maintained in order to not lose receiver sensitivity. What is particularly interesting about this result is the fact that it is consistent with the observation that no significant difference is seen in the heterodyne performances of mixers with J_c = 6.5 and 13 kA/cm^2 and $R_{2.0mV}/R_N$ = 60 and 20, respectively.

Note that the increase in the mixers' broadband sensitivities that is obtained with higher current-density junctions is recognized (see Fig. 9(d)). However, for the purpose of this comparison, only the sensitivities in the 0.8-0.96 THz range are considered.

C. Comparison of the 0.88 and 1.04 THz Results

This twin-junction mixer sensitivity model can also be used to compare the relative sensitivities of the 0.88 and 1.04 THz mixers described in this paper. In particular, Fig. 10 presents the calculated sensitivities of 0.88 and 1.04 THz mixers in which the tuning circuit and junction geometries have been fine-tuned to center the mixers' responses on their respective frequency bands. From this plot, it is seen that a large fraction of the difference in the measured sensitivities of the two mixers is attributable to factors that are included in the previously described mixer noise model. These factors include a drop in the junctions' intrinsic conversion efficiencies and an increase in the noise contributions of optical losses with increasing operating frequency. Additionally, because the penetration depth in NbTiN films deposited at 400ºC is expected to be smaller than that of films deposited at room temperature (due to their significantly higher normal-state conductivities), a larger fraction of the radiation in the NbTiN/SiO_2/Al microstrip penetrates into the (resistive) Al wiring layer. Finally, it is noted that the 1.04 THz devices presented here are characterized by a higher-than-expected series resistance in their current-voltage characteristics, which is a sign that the low-temperature conductivity of the Al wiring layer is likely lower than the $\sigma_{Al,4K}$ = 2-3 x 10^8 Ω^{-1}m^{-1} that is

realized in the 0.88 THz devices.

VIII. Conclusion

The development of SIS mixer devices incorporating NbTiN/SiO_2/Al microstrip tuning circuits and a parallel pair of "standard" 1-μm^2 Nb/Al-AlO_x/Nb SIS junctions has enabled the development of low-noise mixers in the 0.8-1.12 THz range. Furthermore, the use of half-height 0.88 and 1.04 THz waveguide embedding geometries and the optimization of SIS devices to couple efficiently to these embedding circuits has yielded low receiver noise temperatures across the 0.8-0.96 and 0.96-1.12 THz bands of the HIFI instrument; a high-resolution heterodyne spectrometer that is being built for the European Space Agency's Herschel Space Observatory.

Analyzing the measured mixer performance with a three-port admittance and noise model of the SIS tuning circuit (in which 3-port "Tucker" models of the SIS junctions are combined with lumped-element representations of the microstrip transmission lines), it is found that the frequency-dependence of the measured performance is consistent with calculations, but that the measured noise can only be reproduced by inserting 2.8-dB of excess loss into the noise model (in front of the mixer, at a physical temperature of 2.5 K). The calculated results are also consistent with the observation that mixers containing junctions with current-densities of J_c = 6.5 and 13 kA/cm^2 yield similar sensitivities. This may be attributed to the fact that the improved RF coupling that is obtained with higher current-density junctions is offset by an increase in junction shot-noise (due to the fact that the higher current-density junctions have larger leakage currents – $R_{2.0mV}/R_N \sim 20$ for J_c = 13 kA/cm^2 vs $R_{2.0mV}/R_N$ = 30-60 for J_c = 6.5 kA/cm^2)

Finally, a significant fraction of the drop in sensitivity of the 1.04 THz devices relative to the 0.88 THz devices is attributed to the intrinsic effects of the higher operating frequency (which causes the conversion gains of the SIS junctions to drop and the noise contributions of RF losses to increase) and the smaller penetration depth in the "higher quality" NbTiN films used in these devices.

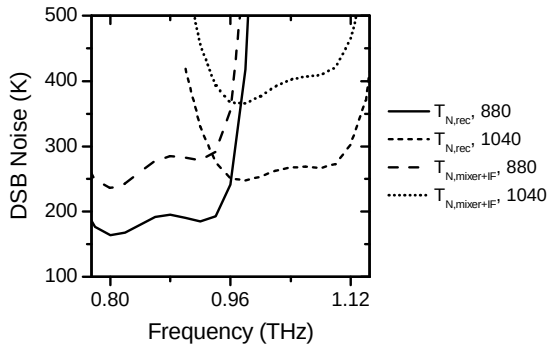

Fig. 10 – Calculated receiver and mixer sensitivities ($T_{N,rec}$ and $T_{N,mixer+IF}$) for 0.88 and 1.04 THz mixers with current-densities of J_c = 6.5 kA/cm^2 and junction qualities of $R_{2.0mV}/R_N$ = 60. The lower sensitivity of the 1.04 THz mixers is due to a combination of the increased operating frequency (which increases the noise contributions of RF coupling losses and reduces the intrinsic conversion efficiency of the junctions) and the reduced coupling efficiency of the tuning circuit (due to the use of a NbTiN ground plane with a higher conductivity, and thus a smaller penetration depth). (In particular, this reduced penetration depth of the NbTiN ground plane causes a larger fraction of the energy in the tuning circuit to penetrate into the Al wiring layer.)

Acknowledgment

The authors would like to thank W. Laauwen and L. de Jong for performing the mixer measurements described here; M. Eggens, H. Golstein, S. Kikken, D. Nguyen, C. Pieters, H. Schaeffer, and H. Smit for their contributions to the design and construction of the mixers and test systems that were used in this work; and A. Baryshev, J.R. Gao, Th. de Graauw, N. Honingh, R. LeDuc, B. Leone, S. Shitov, N. Whyborn, and J. Zmuidzinas for useful discussions.

References

[1] Th. de Graauw and F. P. Helmich on behalf of the HIFI consortium, "Herschel-HIFI: The heterodyne instrument for the far infrared," in *SP-460 The Promise of the Herschel Space Observatory*, G. L. Pilbratt, J. Cernicharo, A. M. Heras, T. Prusti, and R. A Harris, Eds. The Netherlands: ESA, 2001, pp. 45-52.

[2] The HIFI web-site: http://www.sron.nl/divisions/lea/hifi.

[3] G. L. Pilbratt, J. Cernicharo, A. M. Heras, T. Prusti, and R. A Harris, *SP-460 The Promise of the Herschel Space Observatory*. The Netherlands: ESA, 2001.

[4] The Herschel web-site: http://astro.esa.int/herschel.

[5] J. W. Kooi, M. Chan, B. Bumble, H. G. LeDuc, P. Schaffer, and T. G. Phillips, "230 and 492 GHz low noise SIS waveguide receivers employing tuned Nb/AlO_x/Nb tunnel junctions," Int. J. IR and MM Waves, vol. 16, pp. 2049-2068, Dec. 1995.

[6] A. Karpov, J. Blondel, M. Voss, and K. H. Gundlach, "A three photon noise SIS heterodyne receiver at submillimeter wavelength," IEEE Trans. Appl. Superconduct., vol. 9, pp. 4456-4459, June1999.

[7] C. E. Honingh, S. Haas, D. Hottgenroth, K. Jacobs, and J. Stutzki, "Low noise broadband fixed tuned SIS waveguide mixers at 660 and 800 GHz," IEEE Trans. Appl. Superconduct., vol. 7, pp. 2582-2586, June 1997.

[8] D. C. Mattis and J. Bardeen, "Theory of the anomalous skin effect in normal and superconducting metals," Phys. Rev., vol. 111, pp. 412-417, 1958.

[9] G. de Lange, J. J. Kuipers, T. M. Klapwijk, R. A. Panhuyzen, H. van de Stadt, and M. W. M. de Graauw, "Superconducting resonator circuits at frequencies above the gap frequency," J. Appl. Phys., vol. 77, pp. 1795-1804, Dec. 1994.

[10] J. Kawamura, Jian-Chen, D. Miller, J. Kooi, J. Zmuidzinas, B. Bumble, H. G. Leduc, and J. A. Stern, "Low-noise submillimeter-wave NbTiN superconducting tunnel junction mixers," Appl. Phys. Lett., vol. 75, pp. 4013-4015, Dec. 1999.

[11] B. D. Jackson, A. M. Baryshev, G. de Lange, S. V. Shitov, J.-R. Gao, N. N. Iosad, and T. M. Klapwijk, "Low-noise 1 THz superconductor-insulator-superconductor mixer incorporating a NbTiN/SiO_2/Al tuning circuit," Appl. Phys. Lett., vol. 79, pp. 436-438, July 2001.

[12] B. D. Jackson, N. N. Iosad, G. de Lange, A. M. Baryshev, W. M. Laauwen, J.-R. Gao, and T. M. Klapwijk, "NbTiN/SiO_2/Al tuning circuits for low-noise 1 THz SIS mixers," IEEE Trans. Appl. Superconduct., vol. 11, pp. 653-656, March 2001.

[13] B. D. Jackson, G. de Lange, T. Zijlstra, M. Kroug, T. M. Klapwijk, and J. A. Stern, "Niobium titanium nitride based superconductor-insulator-superconductor mixers for low-noise THz receivers," J. Appl. Phys., submitted for publication.

[14] G. de Lange, B. Jackson, T. Zijlstra, M. Kroug, and T.M. Klapwijk, "Development of the band 3 and 4 mixer units for HIFI," in: *Millimeter and Submillimeter Detectors for Astronomy*, edited by Jonas

Zmuidzinas, Wayne S. Holland, Stafford Withington, Proc. of the SPIE Vol. 5498 (SPIE, Bellingham, WA, 2004) pp. 268-277.
[15] J.W. Kooi, unpublished results, 2000-2003.
[16] H. van de Stadt, H. Scheaffer, and L. de Jong, 1996-1998, unpublished.
[17] A. M. Baryshev, H. van de Stadt, H. Schaeffer, R. Hesper, T. Zijlstra, M. Zuiddam, W. Wild, and L. de Jong, "Development of a 0.6 THz SIS receiver for ALMA," in *Proc. 12th Int. Symp. on Space THz Technology*, I. Mehdi, Ed. San Diego, CA: CIT, 2001, pp. 581-590.
[18] Ansoft Corporation, Four Station Square, Suite 2000, Pittsburgh, PA 15219-1119, USA.
[19] J. A. Stern, B. Bumble, H. G. Leduc, J. W. Kooi, and J. Zmuidzinas, "Fabrication and dc-characterization of NbTiN based SIS mixers for use between 600 and 1200 GHz," in *Proc. of the 9th Int. Symp. on Space THz Technology*, R. McGrath, Ed. Pasadena, CA: CIT, 1998, pp. 305-313.
[20] H. B. Callen and T. A. Welton, "Irreversibility and generalized noise," Phys. Rev., vol. 83, pp. 34-40, 1951.
[21] Passive Microwave Technology, Incorporated, 4053 Calle Tesoro, Suite A, Camarillo, CA 93012, USA.
[22] I. Lopez-Fernandez, J. D. Gallego Puyol, A. B. Cancio, and F. Colomer, "New trends in cryogenic HEMT amplifiers for radio astronomy," presented at the Int. Science and Technology Meeting on the Square Kilometer Array, Berkeley, CA, July 9-13, 2001.
[23] J. R. Tucker and M. J. Feldman, "Quantum detection at millimeter wavelengths," Rev. of Mod. Phys., vol. 57, pp. 1055-1113, Oct. 1985.
[24] P. Dieleman, H. G. Bukkems, T. M. Klapwijk, M. Schicke, and K. H. Gundlach, "Observation of Andreev reflection enhanced shot noise," Phys. Rev.Lett., vol. 79, pp. 3486-3489, Nov. 1997.
[25] P. Dieleman and T. M. Klapwijk, "Shot noise beyond the Tucker theory in niobium tunnel junction mixers," Appl. Phys. Lett., vol. 72, pp. 1653-1655, March 1998.

ERROR: undefined
OFFENDING COMMAND:

STACK: